ORIGINAL ARTICLE

Study of Heart Rate Variability to Comprehend the Significance of Singing Bowl Meditation on the Functioning of the Autonomic Nervous System

Ritika Upadhyay [1], Biswajeet Champaty [1*], Suraj Kumar Nayak [2]

[1] *School of Engineering, Ajeenkya DY Patil University, Pune, Maharashtra 412105, India*

[2] *Department of Electrical and Electronics Engineering, School of Engineering and Technology, ADAMAS University, Kolkata, West Bengal, 700126, India*

*Corresponding Author: Biswajeet Champaty
Email: biswajeet.champaty@adypu.edu.in

Received: 06 February 2023 / Accepted: 12 October 2023

Abstract

Purpose: This study aims to determine whether Himalayan singing bowl vibrations could lead to deeper and faster relaxation than supine silence. Numerous civilizations have used singing bowls, gongs, bells, didgeridoos, and voice sounds and chants as instruments for sound healing for ages in religious rites, festivals, social celebrations, and meditation activities.

Materials and Methods: The effect of sound vibrations on physical and mental wellness is supported by scientific research. Although various pieces of research have demonstrated the effect of meditation on humans, very few studies have been done on the beneficial effects of singing bowls on the body and the mind (decrease in unease and temperament, Electroencephalogram, etc.). This study suggests two Machine Learning (ML) models for the automatic classification of the meditative state from the normal state using the Heart Rate Variability (HRV) data.

Results: To pick suitable inputs for the ML models a statistics-based t-test and Principal Component Analysis (PCA) was applied. In the statistics-based t-test method, the HRV parameters were subjected to choose appropriate input for the ML model.

Conclusion: In this case study there are two models that were considered the most effective models based on their accuracy, that are MLP 31-13-2 and RBF 31-17-2 model having a training accuracy of 83.75% and 68.75% respectively. In the second case study, the PCA approach was applied to the HRV parameters, and as a result MLP 4-6-2 and MLP 4-10-2 were the most effective models, with an accuracy of 69.6% and 71.4% respectively.

Keywords: Meditation; Heart Rate Variability; Autonomic Nervous System; Machine Learning; Radial Basis Function.

DOI:

1. Introduction

Meditation, often known as yoga, is a mind-body activity that originates in many different cultures, spiritual societies, and therapeutic methods worldwide. Its origins likely date back more than five thousand years [1]. This complicated physiological procedure affects various neurological, psychological, behavioral, and autonomic roles. This is a different state of perception than wakefulness, slackening at rest, and sleep [2] and is therefore denoted as a transformed state of consciousness [3]. It's possible to meditate in a variety of ways, and the term "meditation" can have a variety of various connotations in different situations. Some of them are Chi, Chakra, Kundalini, Zen, etc.

The harmful effects of anxiety on both the mind and the body are supported by evidence from scientific studies [4, 5]. The effects of stress are not limited to the neurological and endocrine systems; instead, it can also negatively affect cognitive function and the immunological system and lead to an increased risk of developing long-lasting sicknesses [6]. The autonomic nervous system is one of the pathways that is affected by stress. More specifically, the action of the sympathetic nervous system is elevated, while the action of the parasympathetic nervous system is reduced [7, 8].

Since ancient times, significant outcomes have been accredited to the communication of sound with living beings. Notably, specific tools were produced to go together with meditation, and sacred and social rituals, where the sound was utilized to synchronize minds and souls as well as to establish an omnipresent consistency of the entire community throughout earnest festivities [9]. Sound, a bodily vibrational phenomenon that induces reverberation, travels through both audible-ranged and non-audible tissues in the human body. The term "Sound Massage" refers to the awareness of vibration by the entire organism. Remarkably, "Sound Therapy" varies from "Music Therapy" in that "sound" is a perceptible vibration, while "music" is a contrived creation composed of sounds containing harmony, melody, and rhythm [3]. "Sound Therapy" creates the appropriate timbre amongst the vibrations of the singing bells and the pulsation of the individual receiver by using audio like a physical phenomenon with no rhythm or tune. Sound therapists avoid harmonic patterns that may evoke memories of earlier experiences. Gongs and Tibetan Singing Bowls are ancient sound therapy instruments. The resonance of their vibrations determines the ideal mode of sound treatment with the body of the receiver [10, 11].

Several articles [12-15] have reported on the mechanics of Singing Bowls and Gongs. Resonance is described as the instance in which a wavering architecture may engross energy from an exterior source with a high degree of efficiency at only one frequency.

As a stress-reduction method, meditation is commonly referred to as an effective practice. Researchers have paid close attention to the prospective health advantages and impacts on the neuro autonomic function of several meditations and relaxation approaches. According to recent electrophysiological studies, a better understanding of physiology as a whole requires an additional study on the consequences of meditation on physiological states. Most meditation practices affect the Autonomic Nervous System (ANS), indirectly controlling various organs and muscles and their jobs [16]. Heart Rate Variability (HRV) is a metric utilized to quantify Autonomous Nervous System (ANS) functioning. The modifications of the activity of the ANS have been extensively examined using HRV, which is designated by the mining of the bodily rhythms encoded inside its signal. It is difficult to measure HRV because of its non-stability in dynamic situations such as functional testing [17]. When the quantitative and spectral measures of HRV were applied, it was discovered that practicing mindfulness might have diverse consequences on health reliant on the frequencies of the resonant peaks. This finding was made possible as a result of the fact that different meditation techniques produce different HRV patterns [18].

There are very few studies on categorizing meditative and non-meditative states among contemporary techniques. Therefore, this research proposes two different ML techniques that can automatically differentiate between the state of meditation and the regular state by utilizing HRV information. The t-test approach, based on statistical analysis, was applied to the HRV parameters so adequate inputs could be selected for the ML algorithms. Section 2 of this study discusses several

state-of-the-art related works. The methods for the experimental study are presented in section 3. The detailed HRV analysis is described in the next portion of this article. Machine learning model development has been discussed in section 5. The upcoming sections present the outcome of the experimental study and its detailed discussions. Section 8 concludes the study.

One of the most prominent and well-known instances of complicated physiologic variations is the beating of the human heart. The behavior of brain control of the cardiovascular system can be described as complex and nonlinear. According to Bai *et al.* (2008), the constant interaction between sympathetic and parasympathetic nerve processes, which serves to regulate the impulsive beat-to-beat dynamics of cardiac rhythm, is an example of a type of behavior known as nonlinear behavior [19]. Relations are thought to be nonlinear because of the involvement of autonomic nervous system regulation through the physical circumstances on the basis of the dynamic and instantaneous action of the sympathetic and pneumogastric rejoinders to physical environmental tensions [20, 21].

In recent years, meditation has garnered significant interest from researchers in the scientific community. Because of this, the HRV signals have been used to investigate the physiological impact of diverse meditating approaches on the circulatory system. In the past, the dynamics of HRV during the meditative phase were investigated with the help of nonlinear features, such as Hilbert transform [22], Poincare plots [23, 24], dynamical complexity [25], multi-fractal analysis [26], fractal scaling [27], recurrence plot analysis [28], higher-order spectra [29], Lyapunov exponents [30], and wavelet entropy analysis [31]. Conventional Kundalini Yoga and Chinese Chi meditating practices were studied by Peng *et al.* (1999), who used spectrum analysis and a unique analytical-based project upon the Hilbert transform to assess pulse rate patterns linked with deep breathing [22]. When compared to the stage earlier than the meditation control stage, and the other non-meditation control groups, the magnitude of these fluctuations was dramatically increased when seen throughout the meditating stage. Another study by Li *et al.* (2011) on similar meditative practices reveals that, across two distinct types of meditating stages, dynamic complexity diminishes in meditative phases [25]. Furthermore, they found that the spectrum of m-word probabilities shifts throughout the meditating phase, and accounted for this shift by analogy with the sine function's likelihood dispersal. The impact of various latencies upon the breadth of Poincare graphs in cardiac signals throughout meditating state was analyzed by Goshvarpour *et al.* (2011) [23]. They analyzed the Physionet dataset for cardiac signals. Using two separate datasets, the breadth of the Poincare graph was determined for everyone six potential delays. The information reveals that when the delay lengthens, the breadth of the Poincare graph inclines to rise throughout the meditating state. In their study, Song *et al.* (2013) calculated the extent of the singularity intensity among normal youths who practiced Chinese Chi meditating [26]. This allowed researchers to examine the multifractality of cardiac pulse dynamics. They discovered that the multifractal singularity continuum throughout mindfulness practice was substantially shorter than those observed before the meditative phase. This suggests that throughout mindfulness practice, the heart rate becomes frequent, which also demonstrates that the mindfulness practice can assertively alter the regulation of the heart and lungs.

Music-based interventions have been steadily integrated into medical practice [32]. It has been demonstrated that this non-pharmacological therapy can alleviate many symptoms, including agony, nervousness, and tension, and improve pediatric quality of life [33]. In addition, therapeutic effects of music therapy have been described for adults, namely in the setting of clinical depression [34-36] and neurological illnesses [37, 38]. Traditional methods employing acoustic cues due to the introduction of meditative states, like the sound of singing bowls, were further researched [39] as more evidence emerged supporting the therapeutic benefits of the mindfulness concept [40]. Comparing pretreatment parameters to post-treatment parameters using analysis of variance allowed several studies to provide the first perceptions into the biological and spiritual impacts of singing bowl sound [41, 42].

2. Materials and Methods

2.1. Volunteers

Volunteers for the study included 56 ADYPU University undergraduates vacillating in age from 18 to 22 years old. Detailed information about the research work was provided to the participants. The participants agreeing to become a volunteer were requested to fill out a written consent for their involvement in the study. The engagement was completely voluntary, and the already agreed participants were also allowed to cancel their participation in the study if they changed their mood later. The volunteer inclusion conditions comprised of non-occurrence of any cardiac diseases, age group of 18-22 years, and living an active life. The health condition, self-stated by the volunteers based on their earlier health records, was deemed to be correct, and no additional health check-up was carried out.

During the Himalayan Singing Bowls sessions, the participants were instructed to be in a reclining position and close their eyes for fifteen minutes at a time. A Tingsha and seven Himalayan Singing Bowls (Full Moon Singing Bowls) were employed for this experimental study. The diameter of the bowls ranged from 18 centimeters to 29.5 centimeters. The bowls were struck with a mallet (an instrument that looks like a hammer but has a plush, puffed end used for hitting), and there was a minimum gap of five seconds between each succeeding strike. The bowl was initially placed in the position that was furthest from the head, which was between the legs. The bowl's position was gradually changed to one closer to the head, all the time switching sides of the body. The pattern started with a sound with medium intensity (roughly half of the maximum), and the volume was gradually lowered with each succeeding cycle of seven bowl hits and one Tingsha hit (for example, 50%, 40%, etc.). The sequence concluded with a low-intensity sound (about 10% of the maximum). After reaching its minimum level (at 10%), the succeeding cycles gradually raised the intensity until it reached its maximum level (at 50%), and this pattern was repeated for 15 minutes. Following the completion of each cycle was the sound of Tingsha. The participant stayed supine for the entire practice with their eyes closed; however, their eyes were not covered at any point during any of the two types of sessions.

2.2. ECG Signal Acquiring and RR Interval Mining

The student volunteers were requested to make at least one trip to the adjacent ECG recording station to record the ECG signals. It was recommended that the volunteers lie supine on a wooden bed to get the highest level of comfort. Before, during, and after the singing bowl meditation session, the participants' heart rates were monitored with a 12-lead electrocardiogram for a period of five minutes each [43].

The ECG attributes were extracted using the Biomedical Workbench toolbox (National Instruments Corporation, USA). The ECG attribute Extractor first locates the QRS-complexes via the implementation of filtering and rectification in the ECG before moving on to the method for extracting HRV properties. The articles published by National Instruments Corporation stated that the QRS complexes are extracted using a band-pass filter with a 10–25 Hz bandwidth. As a result, during the RR interval (RRI) signal extraction, the information contained in the QRS complexes is considered [44]. The band-pass filter is set up in this manner by default in the software, and it is advised to leave it that way. The default band-pass filter bandwidth of 10-25 Hz was employed in a number of research studies, including Kaur *et al.* (2014), Zaidi *et al.* (2017), Khong *et al.* (2019), and Jain *et al.* (2014) to extract QRS-complexes from ECG signals [45-48]. As a result, during the pre-processing of the ECG, the band-pass filter by a frequency range of 10–25 Hz was utilized. The rectification process can be executed through the absolute or the square technique. In our research, the square technique was used to rectify the preprocessed ECG signals for the extraction of the QRS complexes, followed by the HRV signal.

2.3. HRV Analysis

The typical linear HRV analytic study was executed according to the worldwide recommendations that were published by the mission group of the North American Society of Pacing and Electrophysiology and the European Society of Cardiology [49]. The

linear HRV attributes included the time and frequency arena characteristics [50]. In addition, the nonlinear HRV parameters were determined in accordance with the guidelines provided by the most recent research in the field [51-53]. The Biomedical Workbench toolset of LabVIEW was utilized in the execution of both the linear and nonlinear HRV studies (Figure 1). Every one of the volunteers created a feature vector with a total of 31 different features. Since our study had 56 participants, we were able to generate 56 feature vectors. The testing of hypotheses required the utilization of these feature vectors, which were then utilized in building machine learning models.

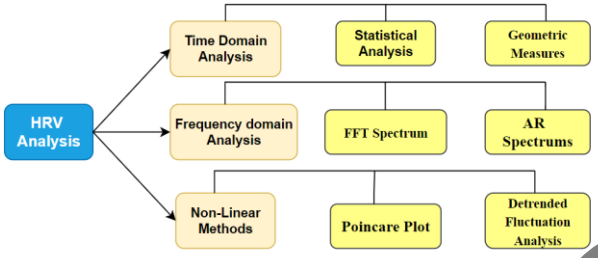

Figure 1. Methods of HRV Analysis

2.3.1. Time-Domain HRV Attributes

The time-domain attributes consist of the features derived from the HRV signals through statistical and geometrical approaches [49]. The time-domain statistical attributes can be determined either straight from the HRV signals or by subtracting them from the RR intermissions [54]. The time-domain statistical attributes, which include the average pulse rate, the standard deviation of the pulse rate, and the average, as well as the standard aberration of the NN intermissions (SD NN), can be derived straight out of those signals (Table 1). In this instance, the attributes HR SD and SD NN disclose data regarding the distribution of the HR and NN interval (or RRI) values from their respective averages. Alternatively, the parameters RMSSD, NN50, and pNN50 provide information about the high-frequency deviation in the heart rate. These parameters are generated from the difference between the RR interludes and show how the heart rate might vary. The root means square standard deviation or RMSSD is the average variation in the interval amid beats and is represented by the square root of the sequential alteration amid the RR intermissions. The value of NN50 provides data about the amount of consecutive NN intermission variances, which had a total period of longer than 50 milliseconds. The value of the parameter pNN50 can be calculated by dividing NN50 by the overall sum of NN intermissions that are longer than 50 milliseconds. TINN, which stands for "triangular interpolation of NN interval histogram," as well as HRV triangular directory are both examples of time-domain geometrical parameters. The HRV triangular index is produced using the RRI histogram (Figure 2). The RRI histogram, also known as the NN interval histogram, can be produced using triangular interpolation. TINN denotes the baseline width of the RRI histogram [55]. We divide the sum of RRIs by the highest value in the RRI histogram to compute the RR triangular index [49].

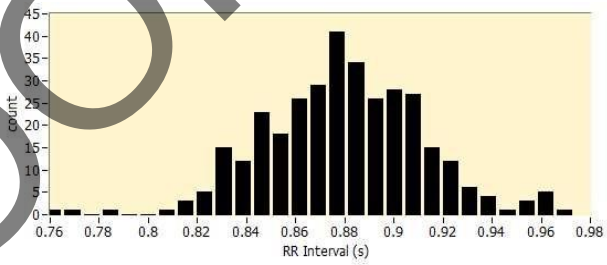

Figure 2. An example of a regular RRI histogram derived from a 5-minute HRV signal. Using the Biomedical Workbench tools that come with LabVIEW, a plot of the RRI distribution was created

2.3.2. Frequency-Domain HRV Attributes

The calculation of the Power Spectral Density (PSD) of the HRV signals serves as the foundation for the frequency domain attributes. Utilizing the Fast Fourier transform (FFT) (Figure 3) and Autoregressive (AR) modeling, the frequency-domain attributes were calculated (Figure 4). Very low frequency of 0-0.04 Hz, low frequency of 0.04-0.15 Hz, and high frequency of 0.15-0.4 Hz components of the PSD were included in the parameters. Typically, absolute power units (ms^2) and related components (percent) are used to quantify the VLF, LF, and HF power components (Table 1). However, the normalized units can also be used to measure the LF and HF components (n.u.). The autonomic modulation of the heart has the potential to change the power dispersal among the numerous components of the

Table 1. Statistical characteristics of significant HRV features t-Test Before and During the Meditation Session

T-Tests Grouping: Category (B & M-HRV parameters sheet-final for analysis)			
Variable	**Mean ± SD**		**p** (< 0.1)
	Without Stimulus (B)	**With Stimulus (M)**	
HF Power-AR	1904.339 ± 973.502	1582.489 ± 984.874	0.084790
LF (%)-AR	33.821 ± 7.732	37.179 ±7.007	0.017720
HF (%)-AR	32.821 ± 8.834	28.929 ±6.246	0.008199
LF/HF-AR	0.737 ± 0.332	0.876 ±0.518	0.093943

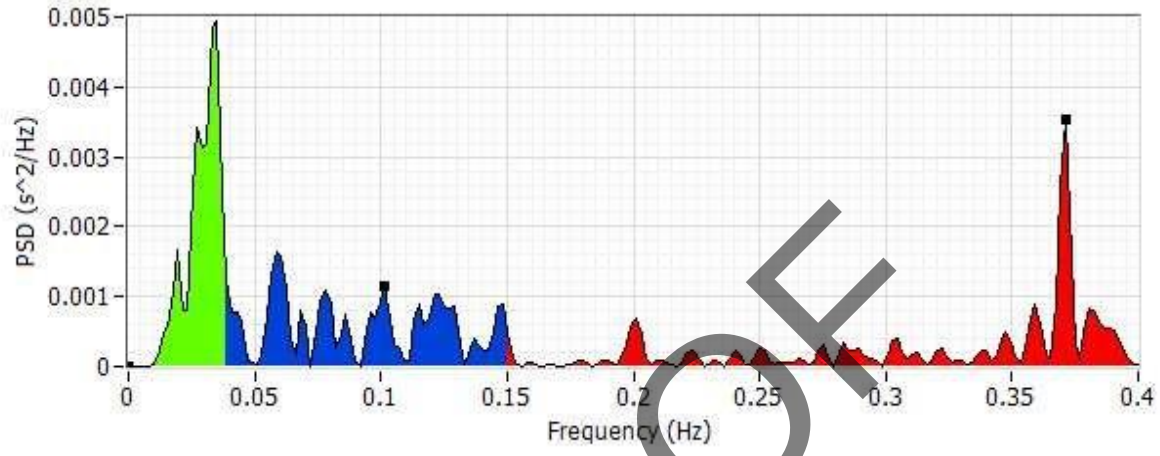

Figure 3. The frequency domain Fourier transform (FFT) band of a 5-minute HRV signal. LabVIEW's Biomedical Workbench package was utilized to generate a graphical representation of the FFT spectrum

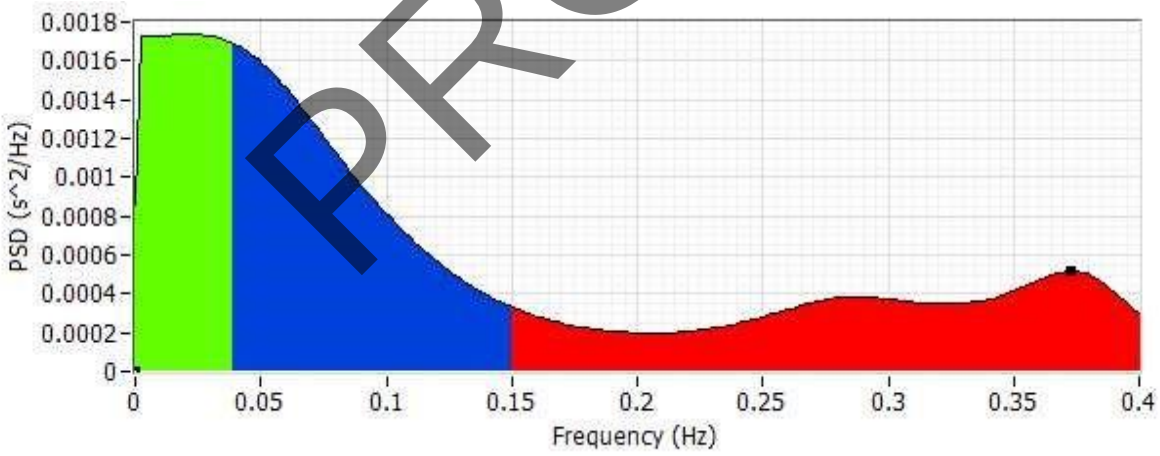

Figure 4. A typical example of an AR spectrum derived from a 5-minute HRV signal. LabVIEW's Biomedical Workbench (National Instruments Corporation, USA) toolset was utilized to generate a plot of the AR spectrum

PSD, which is not static [49]. The precise physiological mechanism generating the VLF power component is not yet known with certainty [49]. The VLF power component is thought to be a sign of parasympathetic activity, but atropine abolishes it [54]. According to some reports, HF power is a sign of parasympathetic action. Nonetheless, the LF power constituent is contrived due to parasympathetic and sympathetic nerve innervations to the Sino-atrial node, which complicates it [54]. Henceforth, the LF/HF proportion is typically utilized in its place of the LF power component unaided to designate the sympathetic actions [54] or the sympathovagal equilibrium [56].

2.3.3. Nonlinear HRV Parameters

Only utilizing linear approaches to describe the HRV is insufficient because the heart is a complex control mechanism. As a result, nonlinear approaches have also been suggested to explain the characteristics of HRV [29] accurately. In this research, the Poincare plot and the Detrended Fluctuation Analysis were used to do the nonlinear HRV analysis (DFA). The Poincare plot illustrates the association amongst the following RRIs in a visual way (Figure 5). Two nonlinear HRV characteristics, SD1 and SD2, are extracted from the data by fitting an ellipse laterally with the line of individuality to the data points (Table 1) [57]. The width and length of the ellipse are used to calculate the parameters SD1 and SD2, respectively. These factors are taken into consideration to be an indicator of both the short-term and the long-term variability, correspondingly [58].

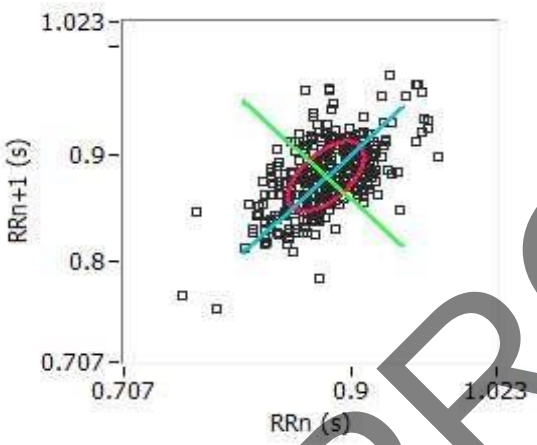

Figure 5. A Poincare plot of a 5-minute HRV signal is presented in the standard format. LabVIEW's Biomedical Workbench was used as the plotting tool for the Poincare diagram

The DFA approach is a nonlinear method for quantifying relationships in any moving functional time series information [59]. In the context of an HRV analytical study, correlations are classified as either short-term or long-term variations, depending on the time frame under consideration. These variations are measured and quantified by the DFA method with the help of the parameters alpha1 (1) and alpha2 (2), respectively (Table 1) [55]. The slope of the log-log graph is employed to determine the values for parameters 1 and 2. These metrics offer a measurement of correlation (in terms of fluctuation Fn) that is dependent on the amount of data that was collected (n) (Figure 6).

2.4. Statistical Analysis

The median (MD), standard deviation (SD), and 25th and 75th percentiles of the values were used to establish the dispersion of HRV characteristics. These actions were taken for both the C and B categories. We used the t-test, implemented with the help of the TIBCO StatSoft Statistica software (StatSoft Europe, 2022), to look into the parameters' statistical significance in light of the data's properties. T-tests are inferential statistics used to examine the possibility of a statistically substantial distinction between the means of two different groups or models and the nature of their correlation [60]. T-tests use the proportion of the variance in means between two categories over the combined standard error of those two groups to estimate the genuine difference between

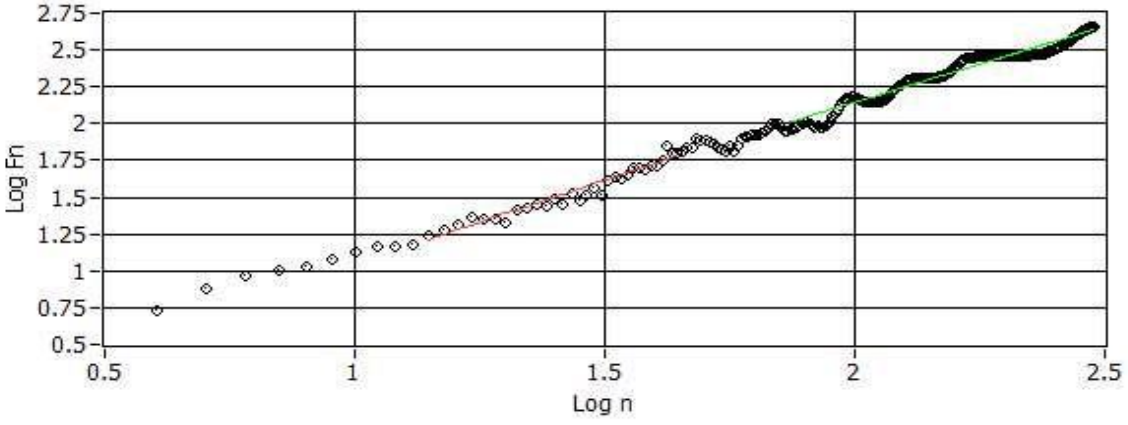

Figure 6. An example representation of a DFA plot using a 5-minute HRV signal. Utilizing the Biomedical Workbench tools (National Instruments Corporation, USA) that is included in LabVIEW, the DFA plot was created

those groups. If the data sets have a normal distribution with unspecified variances, then t-tests can be performed to analyze the data. The calculation of the t-value (t) is presented in Equation 1.

$$t = \frac{\overline{x_1} - \overline{x_2}}{\sqrt{\left(s^2\left(\frac{1}{n_1} + \frac{1}{n_2}\right)\right)}} \quad (1)$$

where x_1 and x_2 depict the average of two categories for comparison, s indicates the standard error between the categories, and n1 and n2 present the number of samples of those categories.

Next, we use the Principal Component Analysis (PCA) method. Data analysis and machine learning both use the dimensionality-reduction method known as Principal Component Analysis (PCA). It is used to reduce the number of dimensions in a high-dimensional dataset while keeping the most significant facts or patterns.

Data standardization is necessary to ensure that each feature in the dataset contributes equally to the analysis. This is especially true if the characteristics in the dataset have varied scales. This entails dividing by the standard deviation for each feature and subtracting the mean for each feature.

To estimate the pairwise covariance between the various features in the dataset, compute the covariance matrix. It divulges details on the connections and interdependencies between the features.

Determine the eigenvalues and eigenvectors: The covariance matrix serves as the source for the eigenvectors and eigenvalues. The eigenvalues quantify the variance explained by each eigenvector, whereas the eigenvectors describe the directions or components with the largest variance in the data.

Finding the principal components—also known as the directions in which the data fluctuates most—is the primary objective of PCA. These major components are orthogonal to one another and ordered according to how much variance in the initial data explained. The mean or average (μ) value of the data samples (xi) can be calculated during the implementation of PCA is given in Equation 2:

$$\mu = \frac{1}{n}\sum_{i=1}^{n}(x_i) \quad (2)$$

where xi represents the data samples

The deviation (ϕ_i) for the data set can be mathematically expressed using Equation 3.

$$\phi_i = x_i - \mu \quad (3)$$

where xi represents the data samples, and μ represents the deviation

2.5. Developing ML Models

Machine learning is a subdivision of computer science that delivers computer learning capability without the necessity for obvious programming [61]. Muti-Layer Perceptron (MLP) and Radial Basis Function (RBF) were utilized for the development of systems that can distinguish the meditative state features of a volunteer in an automatic way using the HRV parameters [62]. These ML methods were applied utilizing the TIBCO StatSoft Statistica software (StatSoft Europe, 2022).

2.5.1. MLP

Multi-Layer Perception (abbreviated as MLP) describes how an individual takes in information from multiple sources. It consists of dense, fully connected layers that may map one dimension to another. Layered neural networks, which create multi-layer perceptions, are a relatively recent development in the field of artificial intelligence. We use a network of neurons in which the outcomes of certain neurons are used as inputs by other neurons to achieve a desired goal.

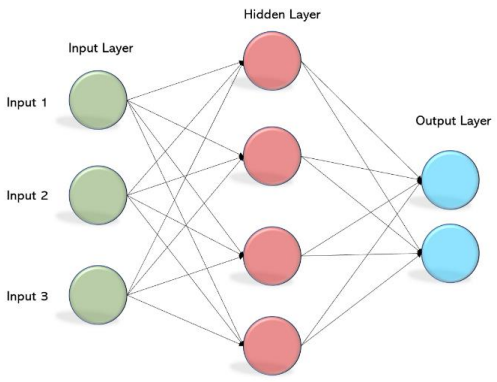

Figure 7. A simple layout of a multi-layer perceptron system [63]

Table 2. Statistical characteristics of significant HRV features t-Test During and After the Meditation session

T-Tests Grouping: Category (M & A-HRV parameters sheet-final for analysis)			
Variable	**Mean ± SD**		**p**(< 0.1)
	With Stimulus (M)	**Without Stimulus (A)**	
RMSSD (ms)	171.339 ± 40.502	187.964±48.295	0.050912
Sd1(ms)	121.393 ± 28.759	133.750±34.659	0.042420
LF (%)-AR	37.179 ± 7.007	34.536±7.628	0.058804
LF n.u.-AR	23.818 ± 7.956	21.009±6.934	0.048897
HF n.u.-AR	46.893 ± 9.164	50.382±11.354	0.076277

2.5.2. RBF

Input, hidden, and an output layer are the components that make up a Radial Basis Function (RBF) neural network. The neurons that make up the hidden layer all have Gaussian transfer functions inside of them, and the outputs of these functions are inversely related to the separation from the neuron's center. The fundamental concept behind this analysis is that an estimated target value for an item is anticipated to be approximately the same as a predicted target value for other objects with quantities of predictors comparable to one another.

3. Results

The research involves collecting the single-lead Electrocardiogram (ECG) signals from 56 volunteers between the ages of 18 to 25, all of whom had to meet certain inclusion criteria and give their written agreement to take part in the research. The mining of the RR intermissions was done utilizing the lead-II ECG signals, and the HRV analysis was executed. The HRV analysis brought about 31 features, which fit into frequency, time, and nonlinear domains. The MD ± SD and the 25th and the 75th percentiles for all the HRV features were calculated from all the groups. Hence, the statistics-based significance of the HRV features was investigated utilizing the statistical technique named the t-test, with a perilous p-value of 0.1. The outcomes recommended that the HF Power-AR, LF (%)-AR, HF (%)-AR, LF/HF-AR, RMSSD, Sd1, LF n.u.-AR, and HF n.u.-AR as the features which fluctuate pointedly among the aforementioned groups. Table 1 presents the statistical characteristics of significant HRV features from the t-test before and during the meditation session. Table 2 shows the statistical characteristics of significant HRV features from the t-test during and after the meditation session.

To simplify the automatic classification of the meditative and normal states employing the HRV information, numerous ML models were developed. The input attributes for the ML methods were selected by the characteristics of the parameters, which had lesser p-values than 0.1. These values were acquired by using a t-test. After that, numerous ML models were established utilizing individual attribute selection techniques based on RBF and MLP neural networks. There were two case studies done in this experimental research. One of the studies was done for 'before' and 'during' the meditation session data, and the other one was done utilizing 'during' and 'after' the meditation session data. We chose the two most suited-valued models out of all those models based on their performances for both case studies. These models came out to be RBF 31-15-2 and MLP 31-13-2 from the first case study (Table 3). From the second case study, we acquired RBF 31-17-2 and MLP 31-7-2 models (Table 4). The software generated the models' training, test, and validation performance values using different error functions, hidden activation, and output activation function values (Tables 3 and 4). The models were evaluated using the models' confusion matrices (Tables 5 and 6).

3.1. Sensitivity

The sensitivity refers to the ability to determine the patient cases correctly. It is estimated as the ratio between accurately classified correct observations to the total number of correct observations. It is also known as a True positive rate or recall.

Table 3. Detailed Construction and Outcomes of the ML Models for Before and During Meditation Data

ML Models	Variables	Training Pref.	Test Pref.	Validation Pref.	Training Algorithm	Error Function	Hidden Activation	Output Activation
RBF 31-15-2	HF Power-AR LF (%)-AR HF (%)-AR LF/HF-AR	50.00%	37.5%	68.75%	RBFT	Entropy	Gaussian	Softmax
MLP 31-13-2	HF Power-AR LF (%)-AR HF (%)-AR LF/HF-AR	83.75%	56.25%	62.50%	BFGS 0	SOS	Exponential	Logistic

Table 4. Detailed Construction and Outcomes of the ML Models for During and After Meditation Data

ML Models	Variables	Training Pref.	Test Pref.	Validation Pref.	Training Algorithm	Error Function	Hidden Activation	Output Activation
RBF 31-17-2	RMSSD Sd1 LF (%)-AR LF n.u.-AR HF n.u.-AR	65.00%	68.75%	56.25%	RBFT	SOS	Gaussian	Identity
MLP 31-7-2	RMSSD Sd1 LF (%)-AR LF n.u.-AR HF n.u.-AR	75.00%	31.25%	62.50%	BFGS 0	SOS	Exponential	Exponential

Table 5. Confusion Matrix for Classifier ANN in Case of Before and During Meditation Data

Model Name	Type	Category-B	Category-M	Category-All
RBF 31-15-2	Total	56.0000	56.0000	112.00000
	Correct	23.0000	34.0000	57.00000
	Incorrect	33.0000	22.0000	55.00000
	Correct (%)	41.0714	60.7143	50.89286
MLP 31-13-2	Total	56.0000	56.0000	112.00000
	Correct	42.0000	44.0000	86.00000
	Incorrect	14.0000	12.0000	26.00000
	Correct (%)	75.0000	78.5714	76.78571

Table 6. Confusion Matrix for Classifier ANN in Case of During and After Meditation Data

Model Name	Type	Category-B	Category-M	Category-All
RBF 31-17-2	Total	56.000000	56.000000	112
	Correct	47.000000	25.000000	72
	Incorrect	9.000000	31.000000	40
	Correct (%)	83.928571	44.642857	64.28
MLP 31-7-2	Total	56.000000	56.000000	112
	Correct	39.000000	36.000000	75
	Incorrect	17.000000	20.000000	37
	Correct (%)	69.642857	64.285714	66.96

Table 7. Detailed Construction and Outcomes of the ML Models for Before and During Meditation Data Using PCA

ML Models	Training Pref.	Test Pref.	Validation Pref.	Training Algorithm	Error Function	Hidden Activation	Output Activation
RBF 4-18-2	73.75000	81.25000	62.50000	RBFT	Entropy	Gaussian	Softmax
MLP 4-8-2	72.50000	62.50000	62.50000	BFGS 0	Entropy	Tanh	Softmax
RBF 4-19-2	48.75000	62.50000	56.25000	RBFT	Entropy	Gaussian	Softmax
MLP 4-9-2	77.50000	68.75000	62.50000	BFGS 36	SOS	Tanh	Logistic
RBF 4-17-2	65.00000	25.00000	56.25000	RBFT	SOS	Gaussian	Identity

Table 8. Detailed Construction and Outcomes of the ML Models for During and After Meditation Data Using PCA

ML Models	Training Pref.	Test Pref.	Validation Pref.	Training Algorithm	Error Function	Hidden Activation	Output Activation
MLP 4-6-2	58.75000	62.50000	43.75000	BFGS 7	Entropy	Exponential	Softmax
MLP 4-6-2	63.75000	68.75000	56.25000	BFGS 11	SOS	Exponential	Identity
RBF 4-15-2	51.25000	31.25000	56.25000	RBFT	SOS	Gaussian	Identity
MLP 4-6-2	71.25000	75.00000	56.25000	BFGS 37	SOS	Logistic	Identity
RBF 4-19-2	55.00000	43.75000	62.50000	RBFT	Entropy	Gaussian	Softmax

Table 9. Confusion Matrix for Classifier ANN in Case of Before and During Meditation Data Using PCA

Model Name	Type	Category-B	Category-M	Category-All
MLP 4-6-2	Total	56.000000	56.000000	112.0000
	Correct	43.000000	35.00000	78.0000
	Incorrect	13.000000	21.00000	34.0000
	Correct (%)	76.78571	62.50000	69.6429
MLP 4-19-2	Total	56.000000	56.00000	112.0000
	Correct	30.000000	31.00000	61.0000
	Incorrect	26.000000	25.00000	51.0000
	Correct (%)	53.57143	55.35714	54.4643

Table 10. Confusion Matrix for Classifier ANN in Case of During and After Meditation Data Using PCA

Model Name	Type	Category-B	Category-M	Category-All
RBF 4-19-2	Total	56.000000	56.000000	112.0000
	Correct	41.000000	37.000000	78.0000
	Incorrect	15.000000	19.000000	34.0000
	Correct (%)	73.21429	66.07143	69.6429
MLP 4-10-2	Total	56.000000	56.000000	112.0000
	Correct	42.000000	38.000000	80.0000
	Incorrect	14.000000	18.000000	32.0000
	Correct (%)	75.00000	67.85714	71.4286

3.2. Sensitivity

The sensitivity refers to the ability to determine the patient cases correctly. It is estimated as the ratio between accurately classified correct observations to the total number of correct observations. It is also known as a True positive rate or recall.

Mathematically, this can be stated as (Equation 4):

$$\text{Sensitivity} = \frac{\text{TP}}{\text{TP} + \text{FN}} \quad (4)$$

where TP and FN refer to the true positive value and the false negative value, respectively.

So, it is important to calculate the sensitivity for all the models like sensitivity for RBF between Category B and D and between Category D and A, also sensitivity for MLP between Category B and D and

between Category D and A. This calculation is also capable of estimating the performance of the machine learning models. Comparing the sensitivity of both the models while dealing with the T-test, it seems that the sensitivity of RBF (between Category B and D) works best with 0.59 whereas RBF (between Category D and Category A) sensitivity falls short with 0.3472. Coming on to MLP, a 0.51 sensitivity of the MLP (between Category B and Category D) was slightly better than the MLP (between Category D and Category A) which was 0.48.

While using PCA, the sensitivity of RBF (between Category B and D) was 0.5 as compared with the 0.47 sensitivity of RBF (between Category D and Category A). Although, both the MLP models, i.e., between Category B and D and between Category D and A sensitivities were almost equal, i.e., 0.44 and 0.47, respectively. Table 11 shows a better understanding of the data.

3.3. Specificity

Specificity corresponds to the ratio of accurately classified negative observations to the total number of negative observations. It is also known as a True Negative Rate (Equation 5).

$$\text{Specificity} = \frac{TN}{TN+FP} \quad (5)$$

where, TN and FP refer to the true negative value and the false positive value, respectively.

Same as sensitivity, specificity was calculated for all four models with the T-test and PCA analysis respectively. In T-test with RBF, there is a substantial improvement in the specificity of RBF (between Category B and D) calculated as 0.6 with respect to RBF (between Category D and A) which was 0.32. But MLP model's specificity was almost neck to neck for both the Categories i.e., 0.53 for Category B and D and 0.45 for Category D and A.

Considering PCA, RBF (between Category B and D) contains a specificity of 0.5 and has greater performance as compared with RBF (between Category D and A) which was 0.44. Moreover, the MLP model between Categories D and A with specificity of 0.43 was preferred over a model between Categories D and A having a specificity of 0.38. Table 12 shows the sensitivity values.

Table 12. Specificity calculated using T-test and PCA models for different Categories

Models	RBF (B and M)	RBF (M and A)	MLP (B and M)	MLP (M and A)
Using T-test	0.6	0.32	0.53	0.45
Using PCA	0.5	0.44	0.43	0.38

4. Discussion

This chapter explored the effects of singing bowls on the physical and psychological states and projected models for the automated classification of the meditative state from the normal state based on their HRV data. The HRV study was executed to identify any changes in the physiological functioning of the ANS. As per the recommendation of the European Society of Cardiology and the North American Society of Pacing and Electrophysiology Committee, the short-term HRV analysis must be executed with at least 5 minutes of ECG sections. This is because the VLF spectral constituent (<5 minutes) of ECG sections may become a questionable measure when it comes to interpreting the power spectral density [49]. Therefore, ECG segments of five minutes were employed to generate the HRV features. The HRV analysis produced a total of 31 features, which were split between the time domain, the frequency domain, and the nonlinear domain. It is an eminent fact that the presence of any variance in the information of the two populaces may be demonstrated from their test specimens (which are of comparatively tiny size) employing hypothesis testing [64]. Statistical methods such as the t-test have been proposed to evaluate hypotheses, provided that the dataset fits the normally distributed plot. In light of this, the statistical method

Table 11. Sensitivity calculated using T-test and PCA models for different categories

Models	RBF (B and M)	RBF (M and A)	MLP (B and M)	MLP (M and A)
Using T-test	0.59	0.34	0.51	0.48
Using PCA	0.5	0.47	0.44	0.47

named the t-test was implemented to identify the HRV properties that substantially differed from one another.

The findings of the t-test (with a critical p-value of 0.1) indicated statistically important HRV features in our study. These attributes are the HF Power-AR, the LF (%)-AR, the HF (%)-AR, the LF/HF-AR, RMSSD, Sd1, LF n.u.-AR, and HF n.u.-AR. We observed that 56 participants' Autonomic Nervous System (ANS) activity varied significantly due to the meditation practiced during singing-bowl sessions. An in-depth analysis of these HRV aspects was performed with the help of the available research literature to understand better the precise variability in the pathophysiology of the ANS. All of the statistically significant HRV attributes had lesser or higher mean and standard deviation values while comparing the before, during, and after the meditation sessions. The average heart rate (HR Mean) was significantly correlated; also, the standard deviation of the heart rate displayed a substantial shift between both the Category-B (Before Mediation), Category M (During Mediation), and Category-C (After Mediation) groups. The properties of the parameters that had p-values that were lower than 0.1 were taken into consideration when deciding which input parameters could be used by the machine learning approaches. The t-test was utilized to obtain these values.

RMSSD is an abbreviation for the root-mean-square of consecutive deviations between regular heartbeats. According to several studies, the reduced levels of RMSSD are greater in healthy populations than in sick populations [70]. The presence of a rise in RMSSD denotes the presence of a rise in PNS. An upsurge in PNS (Parasympathetic Nervous System) parameters is associated with a drop in SNS (Sympathetic Nervous System) activation-related metrics, such as a reduction in heart rate. We can see that this value increases from 171.339 ms with a standard deviation of 40.502 ms to 187.964 with a standard deviation of 48.295 ms after the meditation session.

According to the findings of the t-test analysis, HF n.u AR and LF n.u AR (HF n.u and LF n.u computed utilizing the AR technique) and LF%-AR, HF (%)-AR (LF% and HF% computed utilizing the AR method) are all statistically significant variables. Very Low Frequency (VLF), Low Frequency (LF), and High Frequency (HF) components make the power spectra of the brief-term (e.g., 5-minute) HRV analysis. These components are represented by very low frequency (VLF), low frequency (LF), and high frequency (HF), respectively. In addition to being given in absolute numbers (ms^2), these components are also expressed as a percentage of the overall power (i.e., VLF%, LF%, and HF%). In addition, the low-frequency and high-frequency power components are articulated in a normalized unit (i.e., LF n.u. and HF n.u.). It has been observed that very low frequency (VLF) power and high frequency (HF) power are both markers of parasympathetic activity. Still, low frequency (LF) power is an indicator of sympathetic activity [65]. Here, the LF (%) AR increases during the meditative session and decreases again after the session. The HF (%) -AR value decreases during the session. LF n.u. and HF n.u. values decrease after the session ends. HF power obtained through the AR method honestly represents vagal control of the heart rate [68]. During our case study, we found that the HF power calculated using the AR method declines during the meditation session.

LF/HF-AR is the proportion of the LF band power to the HF band power of AR. The proportion of LF to HF changed based on the patient's heart rate, being lower for reduced heart rates and higher for rapid heart rates. Therefore, the heart's pace can alter LF/HF independently of variations in the activity of the cardiac autonomic nerves [69]. In our case study, during the meditation session, this parameter value increases.

In its most basic form, the Poincare plot is a graphic depiction that compares the present RR intermissions to its previous one [66]. This figure was adjusted using the ellipse-fitting method, which resulted in the generation of three indicators: SD1, SD2, and the proportion of SD1/SD2 (SD12). SD1 is the instant beat-to-beat interval changeability's standard deviation. In contrast hand, SD2 is representative of the persistent long-term abnormalities in the RR interval. The Poincare plot has seen a lot of use in recent years for analyzing the behavior of the ANS. Indicators of parasympathetic modulation have been found for SD1, while an inverse function of sympathetic activation has been considered for SD2 [66, 67]. In this study, we found that SD1 shows an increased value "*after*" the meditation than that of "*during*" the meditative session. In gist, the in-depth

interpretation of the HRV analysis recommended that the HRV parameters show various changes *during* and *after* the meditation session.

ML techniques are increasingly being used as independent decision-making tools for a variety of biomedical applications these days [70]. This chapter aims to present an effective ML algorithm for the classification of meditative and normal states using HRV information collected from individuals who have participated in Himalayan Singing Bowl sessions. Selecting a small set of highly discriminant features is crucial to an ML model's design and modifications [71]. The reason is that the simpler models require fewer features as it simplifies the theoretical difficulties of the feature set. As a bonus, it reduces the overall signal noise level [71]. Several ML systems were created utilizing individual feature selection approaches based on RBF and MLP neural networks. In the course of this experimental investigation, two case studies were carried out. The first study collected data 'before' and 'during' meditation sessions, while the second collected data 'during' and 'after'. Both sets of data were used to analyze the effects of meditation. Out of all those models, we narrowed our selection down to the two that offered the best combination of appropriateness and value. This was done by comparing how well each model performed in both case studies.

So, a statistical technique like a t-test is implemented to figure out the features that ought to be utilized to create ML models. The characteristics that were selected from each method were used to construct and test several different machine-learning models. Of all the models, 4 showed an accuracy of at least 55% (Tables 3 and 4). Therefore, those were the ones that were put through additional inspection so that we could pick the best model. According to the results, we can see that the model based on RBFT neurons (RBF 31-15-2) developed using Gaussian hidden activation and SoftMax output activation shows an inferior performance to that of the MLP 31-15-2 model. MLP 31-15-2 model was created using an exponential as hidden activation with a logistic output activation. This approach presents a training accuracy of 83.75% and a validation accuracy of 62.50%. As a result, this model has been suggested for automatically classifying the HRV data pertaining to the meditative state over the normal condition 'before' and 'during' the meditative session case study. On the other hand, two significant models came out of the experimental study for the second case study, whose input data was accumulated during and after the meditation session. One model, RBF 31-17-2, formed utilizing the RBFT approach with Gaussian activation in the hidden layer and Identity as output activation, showed an accuracy of 65% during training and 56.25% during validation. Similarly, another model named MLP 31-7-2 was created based on the BFGS technique with exponential hidden and output functions, but this model showed a superior output with a training accuracy of 75% and 62.50% during validation. So, it is preferred for the second case study [72].

Finally, the popular dimensionality reduction method PCA was implemented to understand its suitability in finding the various changes occurring in the HRV signal behavior before, during, and after the meditation. While using PCA approach an accuracy of 69.6% and 59.4 % was depicted from the models MLP 4-6-2 and RBF 4-19-2 respectively when before and after meditation data was considered. Whereas, an accuracy of 69.6% and 71.4% obtained from the models RBF 4-19-2 and MLP 4-10-2 respectively when during mediation and after meditation data was considered.

5. Conclusion

The main objective of this study was to identify the existence of changes in the ANS activities due to singing bowl meditation. To the best of our knowledge, this study is the 1st study that has established the use of in-depth HRV analysis for understanding the impact of singing bowl meditation on ANS activity. The results reported in this study will guide future researchers in deep diving into further analysis of singing bowl meditation. In addition, an effort was put forth to come up with an effective ML model for the automatic categorization of the meditation state as opposed to the regular state using the HRV data that had been collected. A p-value check was implemented to choose the input features for said ML algorithms (RBF and MLP). The statistical technique known as the t-test was used to determine which HRV characteristics were significantly distinct from one another. Based on the comparison of all of the models' performance metrics, it appeared that the

MLP 31-13-2 model developed by utilizing the input features chosen via the t-test approach having a training accuracy of 83.75% was the most effective model for prediction for the first case study. The RBF 31-17-2 model was the best approach for the second case study, with a testing accuracy of 68.75%. The classification accuracies reported in this study can be further improved in upcoming studies. Creating ML models was the secondary objective for this study, the main objective being the identification of the existence of changes in the ANS activities due to singing bowl meditation. Hence. our effort for ML model creation to classify the effect of singing bowl meditation can be considered as preliminary work in this regard and the accuracies will be improved further in future studies.

References

1- Ruth A Baer, "Mindfulness training as a clinical intervention: A conceptual and empirical review." *Clinical psychology: Science practice*, Vol. 10 (No. 2), p. 125, (2003).

2- Hans C Lou, Troels W Kjaer, Lars Friberg, Gordon Wildschiodtz, Søren Holm, and Markus Nowak, "A 15O-H2O PET study of meditation and the resting state of normal consciousness." *Human brain mapping*, Vol. 7 (No. 2), pp. 98-105, (1999).

3- Andrew Newberg, Abass Alavi, Michael Baime, Michael Pourdehnad, Jill Santanna, and Eugene d'Aquili, "The measurement of regional cerebral blood flow during the complex cognitive task of meditation: a preliminary SPECT study." *Psychiatry Research: Neuroimaging*, Vol. 106 (No. 2), pp. 113-22, (2001).

4- Agnese Mariotti, "The effects of chronic stress on health: new insights into the molecular mechanisms of brain–body communication." *Future science OA*, Vol. 1 (No. 3), (2015).

5- Peggy A Thoits, "Stress and health: Major findings and policy implications." *Journal of health social behavior*, Vol. 51 (No. 1_suppl), pp. S41-S53, (2010).

6- Mohd Razali Salleh, "Life event, stress and illness." *The Malaysian journal of medical sciences: MJMS*, Vol. 15 (No. 4), p. 9, (2008).

7- Herbert Benson and William Proctor, Relaxation revolution: The science and genetics of mind body healing. *Simon and Schuster*, (2011).

8- Y Trivedi Gunjan, R Hemalatha, and KV Ramani, "Chronic Diseases and Mind Body Management, an Introduction (Technical Note), Reference No: CMHS0044TEC." *Indian Institute of Management*, (2018).

9- Jörg Fachner and Sabine Rittner, "Ethno Therapy, Music and Trance: an EEG investigation into a sound-trance induction." in *States of Consciousness*: *Springer*, (2011), pp. 235-56.

10- Peter Hess, "Singing Bowls for Health and Inner Harmony." *Through Sound MassageAccording to Peter Hess, Germany: DruckereiRindt GmbH, Fulda*, (2008).

11- Luca Pigaiani, Bagno Armonico®-Massaggio sonoro con campane tibetane: Basi teoriche e campi di applicazione. *Fontana Editore*, (2014).

12- Neville H Fletcher and Thomas D Rossing, The physics of musical instruments. *Springer Science & Business Media*, (2012).

13- Thomas D Rossing, Junehee Yoo, and Andrew Morrison, "Acoustics of percussion instruments: An update." *Acoustical science technology*, Vol. 25 (No. 6), pp. 406-12, (2004).

14- Octávio Inácio, Luís Henrique, and José Antunes, "The physics of Tibetan singing bowls." *Revista de Acústica*, Vol. 35pp. 1-2, (2003).

15- Denis Terwagne and John WM Bush, "Tibetan singing bowls." *Nonlinearity*, Vol. 24 (No. 8), p. R51, (2011).

16- Masahito Sakakibara, Satoshi Takeuchi, and Junichiro Hayano, "Effect of relaxation training on cardiac parasympathetic tone." *Psychophysiology*, Vol. 31 (No. 3), pp. 223-28, (1994).

17- Vincent Pichot *et al.*, "Wavelet transform to quantify heart rate variability and to assess its instantaneous changes." *Journal of Applied Physiology*, Vol. 86 (No. 3), pp. 1081-91, (1999).

18- Sukanya Phongsuphap, Yongyuth Pongsupap, Pakorn Chandanamattha, and Chidchanok Lursinsap, "Changes in heart rate variability during concentration meditation." *International journal of cardiology*, Vol. 130 (No. 3), pp. 481-84, (2008).

19- Yan Bai *et al.*, "Nonlinear coupling is absent in acute myocardial patients but not healthy subjects." Vol. 295 (No. 2), pp. H578-H86, (2008).

20- Solange Akselrod, David Gordon, F Andrew Ubel, Daniel C Shannon, A Clifford Berger, and Richard J Cohen, "Power spectrum analysis of heart rate fluctuation: a quantitative probe of beat-to-beat cardiovascular control." *science*, Vol. 213 (No. 4504), pp. 220-22, (1981).

21- Matthew N Levy, "Brief reviews: sympathetic-parasympathetic interactions in the heart." *Circulation research*, Vol. 29 (No. 5), pp. 437-45, (1971).

22- C-K Peng *et al.*, "Exaggerated heart rate oscillations during two meditation techniques." Vol. 70 (No. 2), pp. 101-07, (1999).

23- Atefeh Goshvarpour, Ateke Goshvarpour, and Saeed Rahati, "Analysis of lagged Poincare plots in heart rate

signals during meditation." *Digital Signal Processing*, Vol. 21 (No. 2), pp. 208-14, (2011).

24- Atefeh Goshvarpour and Ateke Goshvarpour, "Poincare indices for analyzing meditative heart rate signals." *Biomedical journal*, Vol. 38 (No. 3), (2015).

25- Jin Li, Jing Hu, Yinhong Zhang, and Xiaofeng Zhang, "Dynamical complexity changes during two forms of meditation." *Physica A: Statistical Mechanics its Applications*, Vol. 390 (No. 12), pp. 2381-87, (2011).

26- Renliang Song, Chunhua Bian, and Qianli DY Ma, "Multifractal analysis of heartbeat dynamics during meditation training." *Physica A: Statistical Mechanics its Applications*, Vol. 392 (No. 8), pp. 1858-62, (2013).

27- J Alvarez-Ramirez, E Rodríguez, and JC Echeverría, "Fractal scaling behavior of heart rate variability in response to meditation techniques." *Chaos, Solitons Fractals*, Vol. 99pp. 57-62, (2017).

28- Ateke Goshvarpour and Atefeh Goshvarpour, "Recurrence plots of heart rate signals during meditation." *International Journal of Image, Graphics Signal Processing*, Vol. 4 (No. 2), p. 44, (2012).

29- Ateke Goshvarpour and Atefeh Goshvarpour, "Comparison of higher order spectra in heart rate signals during two techniques of meditation: Chi and Kundalini meditation." *Cognitive neurodynamics*, Vol. 7 (No. 1), pp. 39-46, (2013).

30- Ateke Goshvarpour and Atefeh Goshvarpour, "Classification of heart rate signals during meditation using Lyapunov exponents and entropy." *Int. J. Intell. Syst. Appl*, Vol. 2pp. 35-41, (2012).

31- Junling Gao *et al.*, "Entrainment of chaotic activities in brain and heart during MBSR mindfulness training." Vol. 616pp. 218-23, (2016).

32- Tamara L Goldsby and Michael E Goldsby, "Eastern integrative medicine and ancient sound healing treatments for stress: recent research advances." *Integrative Medicine: A Clinician's Journal*, Vol. 19 (No. 6), p. 24, (2020).

33- Thomas Stegemann, Monika Geretsegger, Eva Phan Quoc, Hannah Riedl, and Monika Smetana, "Music therapy and other music-based interventions in pediatric health care: An overview." *Medicines*, Vol. 6 (No. 1), p. 25, (2019).

34- Anna Maratos, Christian Gold, Xu Wang, and Mike Crawford, "Music therapy for depression." *Cochrane database of systematic reviews*, (No. 1), (2008).

35- Daniel Leubner and Thilo Hinterberger, "Reviewing the effectiveness of music interventions in treating depression." *Frontiers in psychology*, Vol. 8p. 1109, (2017).

36- Qishou Tang, Zhaohui Huang, Huan Zhou, and Peijie Ye, "Effects of music therapy on depression: A meta-analysis of randomized controlled trials." *Plos one*, Vol. 15 (No. 11), p. e0240862, (2020).

37- Hiroharu Kamioka *et al.*, "Effectiveness of music therapy: a summary of systematic reviews based on randomized controlled trials of music interventions." Vol. 8p. 727, (2014).

38- Tamaya Van Criekinge, Kristiaan D'Août, Jonathon O'Brien, and Eduardo Coutinho, "The influence of sound-based interventions on motor behavior after stroke: A systematic review." *Frontiers in neurology*, Vol. 10p. 1141, (2019).

39- Jessica Stanhope and Philip Weinstein, "The human health effects of singing bowls: A systematic review." *Complementary Therapies in Medicine*, Vol. 51p. 102412, (2020).

40- Stefan G Hofmann and Angelina F Gómez, "Mindfulness-based interventions for anxiety and depression." *Psychiatric clinics*, Vol. 40 (No. 4), pp. 739-49, (2017).

41- Jayan Marie Landry, "Physiological and psychological effects of a Himalayan singing bowl in meditation practice: a quantitative analysis." *American Journal of Health Promotion*, Vol. 28 (No. 5), pp. 306-09, (2014).

42- Tamara L Goldsby, Michael E Goldsby, Mary McWalters, and Paul J Mills, "Effects of singing bowl sound meditation on mood, tension, and well-being: an observational study." *Journal of evidence-based complementary alternative medicine*, Vol. 22 (No. 3), pp. 401-06, (2017).

43- Ary L Goldberger, Zachary D Goldberger, and Alexei Shvilkin, Clinical Electrocardiography: A Simplified Approach E-Book: A Simplified Approach. *Elsevier Health Sciences*, (2017).

44- Max Jaderberg, Andrea Vedaldi, and Andrew Zisserman, "Deep features for text spotting." in *European conference on computer vision*, (2014): *Springer*, pp. 512-28.

45- Poonam Kaur and RK Sharma, "LabVIEW based design of heart disease detection system." in *International Conference on Recent Advances and Innovations in Engineering (ICRAIE-2014)*, (2014): *IEEE*, pp. 1-5.

46- Saket Jain and Piyush Kumar, "LABVIEW based expert system for Detection of heart abnormalities." in *2014 International Conference on Advances in Electrical Engineering (ICAEE)*, (2014): *IEEE*, pp. 1-5.

47- Akib Mohammad Azam Zaidi, Muhammad Jubaer Ahmed, and ASM Bakibillah, "Feature extraction and characterization of cardiovascular arrhythmia and normal sinus rhythm from ECG signals using LabVIEW." in *2017 IEEE International Conference on Imaging, Vision & Pattern Recognition (icIVPR)*, (2017): *IEEE*, pp. 1-6.

48- WL Khong, M Mariappan, and NSV Kameswara Rao, "National Instruments LabVIEW Biomedical Toolkit for Measuring Heart Beat Rate and ECG LEAD II Features."

in *IOP Conference Series: Materials Science and Engineering*, (2019), Vol. 705 (No. 1): *IOP Publishing*, p. 012020.

49- A John Camm *et al.*, "Heart rate variability: standards of measurement, physiological interpretation and clinical use. Task Force of the European Society of Cardiology and the North American Society of Pacing and Electrophysiology." (1996).

50- Fred Shaffer and JP Ginsberg, "An overview of heart rate variability metrics and norms." *Frontiers in public health*, Vol. 5p. 258, (2017).

51- Mimma Nardelli, Alberto Greco, Matteo Bianchi, Enzo Pasquale Scilingo, and Gaetano Valenza, "Classifying affective haptic stimuli through gender-specific heart rate variability nonlinear analysis." *IEEE Transactions on Affective Computing*, (2018).

52- Felipe X Cepeda, Matthew Lapointe, Can Ozan Tan, and J Andrew Taylor, "Inconsistent relation of nonlinear heart rate variability indices to increasing vagal tone in healthy humans." *Autonomic Neuroscience*, Vol. 213pp. 1-7, (2018).

53- Rosangela A Hoshi *et al.*, "Linear and nonlinear analyses of heart rate variability following orthostatism in subclinical hypothyroidism." *Medicine*, Vol. 98 (No. 4), (2019).

54- Robert E Kleiger, Phyllis K Stein, and J Thomas Bigger Jr, "Heart rate variability: measurement and clinical utility." *Annals of Noninvasive Electrocardiology*, Vol. 10 (No. 1), pp. 88-101, (2005).

55- Mika P Tarvainen, Jukka A Lipponen, and Pekka Kuoppa, "Analysis and Preprocessing of HRV—Kubios HRV Software." in *ECG Time Series Variability Analysis*: *CRC Press*, (2017), pp. 159-86.

56- H Nagendra, Vinod Kumar, and Shaktidev Mukherjee, "Cognitive behavior evaluation based on physiological parameters among young healthy subjects with yoga as intervention." *Computational and Mathematical Methods in Medicine*, Vol. 2015(2015).

57- Marina Medina Corrales, Blanca de la Cruz Torres, Alberto Garrido Esquivel, Marco Antonio Garrido Salazar, and José Naranjo Orellana, "Normal values of heart rate variability at rest in a young, healthy and active Mexican population." *Health*, Vol. 4 (No. 7), pp. 720-26, (2012).

58- Mika P Tarvainen, Juha-Pekka Niskanen, Jukka A Lipponen, Perttu O Ranta-Aho, and Pasi A Karjalainen, "Kubios HRV–heart rate variability analysis software." *Computer Methods and Programs in Biomedicine*, Vol. 113 (No. 1), pp. 210-20, (2014).

59- C-K Peng, Shlomo Havlin, H Eugene Stanley, and Ary L Goldberger, "Quantification of scaling exponents and crossover phenomena in nonstationary heartbeat time series." *Chaos: An Interdisciplinary Journal of Nonlinear Science*, Vol. 5 (No. 1), pp. 82-87, (1995).

60- Doug Semenick, "Tests and measurements: The T-test." *Strength Conditioning Journal*, Vol. 12 (No. 1), pp. 36-37, (1990).

61- Claude Sammut and Geoffrey I Webb, Encyclopedia of machine learning and data mining. *Springer Publishing Company, Incorporated*, (2017).

62- Vijay Kotu and Bala Deshpande, Predictive analytics and data mining: concepts and practice with rapidminer. *Morgan Kaufmann*, (2014).

63- Awhan Mohanty. (2019). Multi layer Perceptron (MLP) Models on Real World Banking Data. [Online]. Available: https://becominghuman.ai/multi-layer-perceptron-mlp-models-on-real-world-banking-data-f6dd3d7e998f.

64- David G Rees, Essential statistics. *Chapman and Hall/CRC*, (2018).

65- Zhiping Niu *et al.*, "Acute effect of ambient fine particulate matter on heart rate variability: an updated systematic review and meta-analysis of panel studies." *Environmental health preventive medicine*, Vol. 25 (No. 1), pp. 1-15, (2020).

66- Shr-Da Wu and Pei-Chen Lo, "Inward-attention meditation increases parasympathetic activity: a study based on heart rate variability." *Biomedical Research*, Vol. 29 (No. 5), pp. 245-50, (2008).

67- Goncalo Vilhena Mendonca, Bo Fernhall, Kevin S Heffernan, and Fernando D Pereira, "Spectral methods of heart rate variability analysis during dynamic exercise." *Clinical Autonomic Research*, Vol. 19 (No. 4), pp. 237-45, (2009).

68- George E Billman, "The LF/HF ratio does not accurately measure cardiac sympatho-vagal balance." Vol. 4, ed. Frontiers in physiology: Frontiers Media SA, (2013), p. 26.

69- Peter Walter Kamen, Henry Krum, and Andrew Maxwell Tonkin, "Poincare plot of heart rate variability allows quantitative display of parasympathetic nervous activity in humans." *Clinical science*, Vol. 91 (No. 2), pp. 201-08, (1996).

70- Corrales Marina Medina, Torres Blanca de la Cruz, Esquivel Alberto Garrido, Salazar Marco Antonio Garrido, and Naranjo Orellana José, "Normal values of heart rate variability at rest in a young, healthy and active Mexican population." *Health*, Vol. 2012(2012).

71- Alvin Rajkomar, Jeffrey Dean, and Isaac Kohane, "Machine learning in medicine." *New England Journal of Medicine*, Vol. 380 (No. 14), pp. 1347-58, (2019).

72- Robert Nisbet, John Elder, and Gary Miner, Handbook of statistical analysis and data mining applications. *Academic Press*, (2009).